

A compact and low-loss polarization splitter based on dual-core photonic crystal fiber

Chao Dou^{1,2} · Xili Jing¹ · Shuguang Li¹ · Junjun Wu^{1,3} · Qingbo Wang^{1,4}

Received: 23 December 2017 / Accepted: 28 May 2018 / Published online: 7 June 2018
© Springer Science+Business Media, LLC, part of Springer Nature 2018

Abstract The characteristics of a novel dual-core photonic crystal fiber are investigated. In the center of photonic crystal fiber, an energy transmission channel is introduced. The optimized photonic crystal fiber can be used for polarization splitter, which has a short length and low loss.

Keywords Photonic crystal fiber · Polarization splitter · Extinction ratio · Insertion loss

1 Introduction

When the light is transmitted in a single-mode fiber, there are two mutually perpendicular intrinsic polarization modes in the fiber. Due to the elliptical deformation of the core and the residual internal stress, the fiber always exhibits birefringence in practice. As a result, the two polarization states of the fundamental mode are no longer degenerate, and they propagate at different velocities. It may lead to the pulse broadening and signal distortion, which limits the transmission bandwidth of the system. A polarization device could be used to avoid the aforementioned problems. Although the polarization devices based on the traditional optical fiber have been applied in practical for a long time (Miliou et al. 1993; Wu et al. 1995; Peng et al. 1990), they have some defects such as long length and narrow

✉ Xili Jing
sljingxl@ysu.edu.cn

¹ Key Laboratory for Microstructural Material Physics of Hebei Province, School of Science, Yanshan University, Qinhuangdao 066004, People's Republic of China

² Department of Basic Education, Tangshan University, Tangshan 063000, People's Republic of China

³ College of Qing Gong, North China University of Science and Technology, Tangshan 063009, People's Republic of China

⁴ Department of Physics, Tangshan Normal University, Tangshan 063000, People's Republic of China

working bandwidth. Since optical fiber communications evolve toward the large capacity and integration, more compacted polarization devices are desired.

In recent years, new photonic crystal fiber (PCF) has been used in the polarization devices, and many excellent products have sprung up. On one hand, the structure of PCF is flexible and adjustable, such as the diameters, pitch and arrangement of the air holes, the size and shape of the core area (Fan et al. 2014; Liu et al. 2015; Wu et al. 2013; Li and Zhou 2016; Yogalakshmi et al. 2016). By adjusting the diameter of dual-core tellurite glass photonic crystal fiber, Fan et al. (2014) obtained a polarization beam splitter with high extinction ratios at the wavelengths of 1.33 and 1.55 μm . Liu et al. (2015) proposed a polarization splitter based on square-lattice ZnTe glass PCF, with the fiber length of 1.1452 mm. On the other hand, by selectively filling or coating metal in the holes of PCF, the plasma wave is only stimulated by a certain polarization state, which is an ideal attribute that can be used in the polarizing filters and splitters (Li and Zhao 2013; Nagasaki et al. 2011; Khaleque and Hattori 2015; Schmidt et al. 2008). Nagasaki et al. (2011) investigated the effect of the filling position of the metal wires on the polarization characteristics. Khaleque and Hattori (2015) proposed a polarizer based on a squeezed rectangular lattice PCF coating with the gold layer, of which the modal losses for the x-polarized mode and y-polarized mode are 1221 and 1.6 dB/cm. However, the output power and the loss of PCF polarizers are rarely reported.

In this paper, we present a novel polarization splitter based on dual-core photonic crystal fiber. The finite element method (FEM) is utilized to investigate the polarization-dependent coupling in dual-core PCF. By changing the diameters and pitch of the air holes, we get the optimum coupling lengths of x- and y-polarization state for the 1.55 μm polarization splitter. The performance of the polarization splitter is evaluated.

2 Basic theory and original structure

The cross section of the PCF we proposed is shown in Fig. 1. The background material of the fiber is pure silica, whose dispersion relationship is calculated by the Sellmeier equation (Geng et al. 2012). The air holes consist of two kinds of circular holes and two elliptic holes, which are arranged in a rectangular lattice. The diameter of the big circular holes is denoted by d_1 , and the spacing between big circular holes is denoted by Λ_1 . The diameter of the small circular holes is denoted by d_2 , and the spacing between the adjacent big and small circular holes is denoted by Λ_2 . The long axis of two elliptic holes is denoted by \mathbf{a} , and the short axis is denoted by \mathbf{b} . Two circular holes in x-direction are taken out to form core A and core B. The original parameters of PCF are: $d_1 = 2 \mu\text{m}$, $d_2 = 1 \mu\text{m}$, $\Lambda_1 = 2.5 \mu\text{m}$, $\Lambda_2 = 2 \mu\text{m}$, $\mathbf{a} = 2 \mu\text{m}$, $\mathbf{b} = 1 \mu\text{m}$.

PCFs used for polarization splitter always have high birefringence, the coupling lengths of x- and y-polarized state are defined as (Florous et al. 2005)

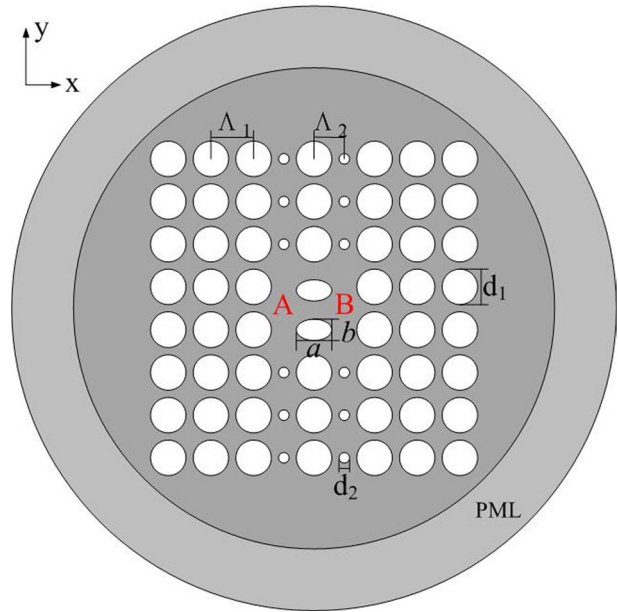
$$L_{x,y} = \frac{\lambda}{2(n_{\text{even}}^{x,y} - n_{\text{odd}}^{x,y})} \quad (1)$$

where λ is the wavelength in free space.

Assumed that the input power is pumped into core A, the output power of x- and y-polarized state in core A can be calculated as (Florous et al. 2005)

$$P_{\text{out}}^{x,y} = P_{\text{in}} \cos^2 \left(\frac{\pi \cdot L}{2L_{x,y}} \right) \quad (2)$$

Fig. 1 Cross section of the designed polarization splitter



Similarly, the output power of x- and y-polarized state in core B can be calculated as (Florous et al. 2005)

$$P_{out}^{x,y} = P_{in} \sin^2 \left(\frac{\pi \cdot L}{2L_{x,y}} \right) \tag{3}$$

L stands for the propagation distance.

When the values meet the condition of $L = mL_x = nL_y$, where m and n are positive integers and their parity are different, the two polarized states in the cores can be separated.

The crosstalk between different polarization states can be assessed by the extinction ratios (ER). ER_A and ER_B are defined as (Jiang et al. 2014)

$$ER_A = 10 \log_{10} \left(\frac{P_A^y}{P_A^x} \right) \tag{4}$$

$$ER_B = 10 \log_{10} \left(\frac{P_B^x}{P_B^y} \right) \tag{5}$$

where P_A^x is the output power of x-polarized mode in core A, P_A^y is the output power of y-polarized mode in core A; P_B^x is the output power of x-polarized mode in core B, P_B^y is the output power of y-polarized mode in core B.

When the extinction ratio is less than -20 dB, the output power ratio of two polarization modes is greater than 100, two polarization modes can be separated very well (Jiang et al. 2014).

3 Simulation process and numerical analysis

The simulation software is Comsol Multiphysics, and finite element method (FEM) is utilized to calculate the characteristics of PCF. Scattering boundary conditions are employed in the simulation process, and the thickness of perfect matched layer (PML) is set to be $3\ \mu\text{m}$. Figure 2 shows the electrical field distribution of fundamental modes in x- and y-polarized direction, including two odd modes (Fig. 2a, c) and two even modes (Fig. 2b, d). Core A and core B are separated by two elliptical holes in the center of PCF. Due to the short axes of two elliptical holes are located in the y-direction, a channel is formed in the area between two elliptical holes for energy transmission. Compared to Fig. 2d, the energy in Fig. 2b is more easily transferred between two core areas.

Figure 3 shows the effective refractive indexes of four polarization modes, the descending order is x-even mode, y-even mode, y-odd mode and x-odd mode. Due to the structure asymmetry of the PCF, the refractive index difference between x-odd mode and x-even mode is significantly bigger than that between y-odd mode and y-even mode.

3.1 Structure optimization

Figure 4 depicts the effect of hole spacing on the coupling lengths. L_x and L_y are the coupling lengths of x- and y-polarization mode at the wavelength of $1.55\ \mu\text{m}$. When the spacing (denoted by Λ_1) between large circular holes changes to 2.2, 2.3, 2.4, 2.5 μm , the spacing (denoted by Λ_2) between the adjacent large and small circular holes changes to 1.7, 1.8, 1.9, 2.0 μm , correspondingly. As increasing Λ_1 and Λ_2 , the mode fields of core A and core

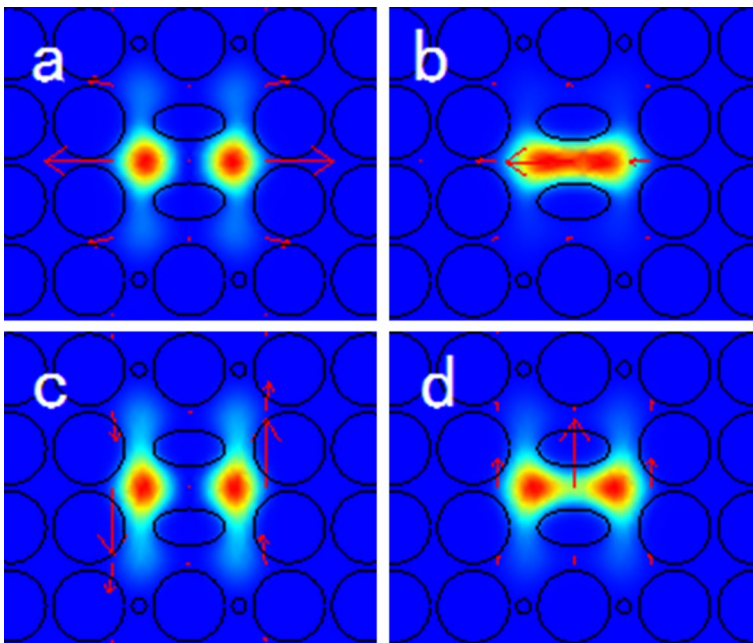


Fig. 2 Electrical field distributions at the wavelength of $1.55\ \mu\text{m}$ for **a** x-odd mode, **b** x-even mode, **c** y-odd mode, **d** y-even mode

Fig. 3 Effective refractive indexes of four polarization modes vary with wavelength

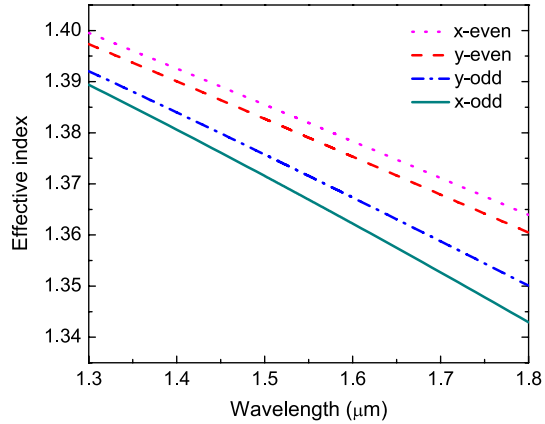
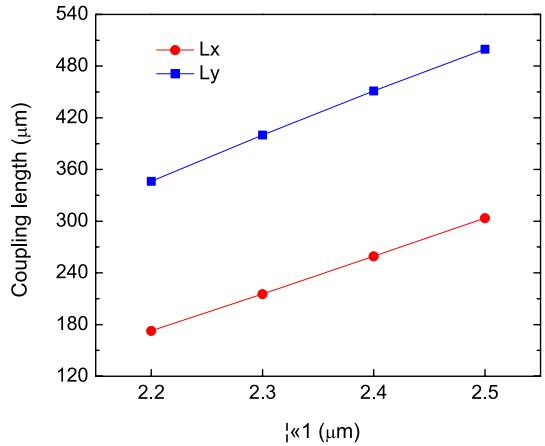


Fig. 4 Coupling lengths vary with the spacing between big circular holes



B expand and the energy becomes divergent. This change increases the difficulty of the mode coupling and leads to the increase of L_x and L_y . In order to obtain smaller coupling lengths, we reduce the values of A_1 and A_2 : $A_1 = 2.2 \mu\text{m}$ and $A_2 = 1.7 \mu\text{m}$.

For the purpose of improving the birefringence of PCF, we introduce two columns of small circular holes on both sides of the elliptical holes. The diameter of small circular holes (denoted by d_2) is changed to 0.4, 0.6, 0.8, 1.0, 1.2, 1.4 μm , in turn. Figure 5 shows when d_2 is 0.4 μm , L_x is 50 μm and L_y is 99 μm ; when d_2 is 1.4 μm , L_x is 332 μm and L_y is 627 μm . L_x and L_y obviously increase as d_2 increasing. This is because the mode field is enlarged in the x-direction, which increases the difficulty of energy transmission between core A and B. So we optimize the value of d_2 to 0.4 μm .

Figure 6 shows the coupling lengths vary with the short axis length of the elliptical holes (denoted by b). When b increase, the channel between core A and B becomes narrow. It increases the difficulty of the energy transfer between two cores. Thus L_x and L_y increase as b increasing. However, we can not blindly reduce b . The ratio of the coupling lengths should be taken into account at the same time. When b is 1.02 μm , L_x is 51.6 μm and L_y is 103.1 μm , the ratio is 1.998. The ratio is very close to the integer value of 2. So the optimized value of b is 1.02 μm .

Fig. 5 Coupling lengths vary with the diameter of small circular holes

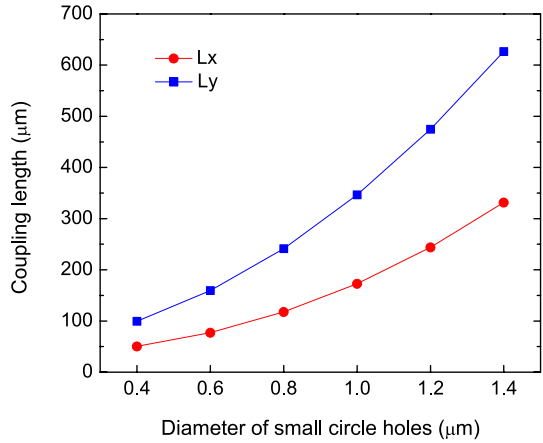
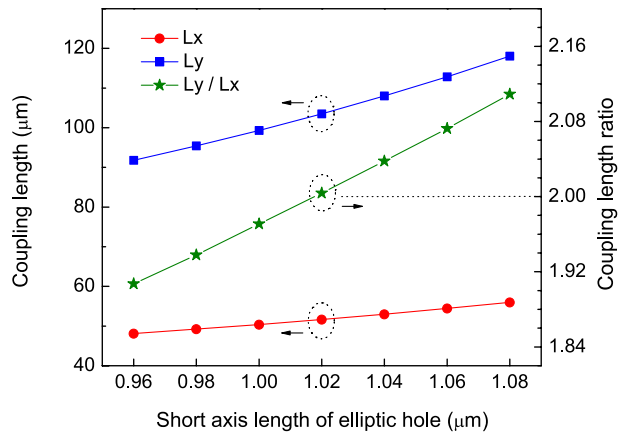


Fig. 6 Coupling length varies with the short axis length of the elliptic holes

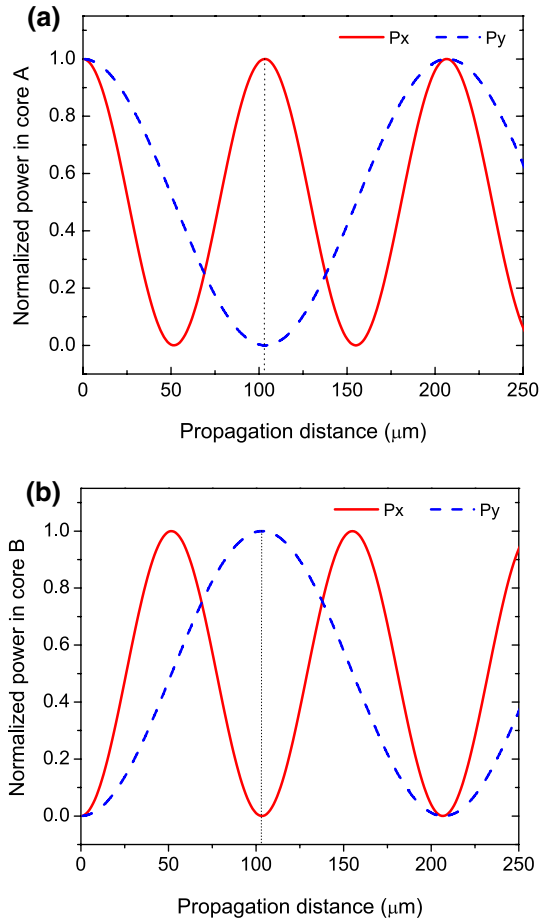


In summary, the optimized parameters of PCF are as follows: $d_1 = 2 \mu\text{m}$, $d_2 = 0.4 \mu\text{m}$, $\Lambda_1 = 2.2 \mu\text{m}$, $\Lambda_2 = 1.4 \mu\text{m}$, $a = 2 \mu\text{m}$, $b = 1.02 \mu\text{m}$.

3.2 Splitting distance and extinction ratio

Assumed that the normalized power pumped into core A is 1, while the normalized power pumped into core B is 0. The length of the polarization splitter is set to $103 \mu\text{m}$ ($L = L_y = 2L_x$), which is an important parameter of polarization splitter. Figure 7a shows that the normalized power in core A depends on the propagation distance, and the curves follow the law of cosine function. When the propagation distance is $103 \mu\text{m}$, P_x is 0.99991 and P_y is 0.00006. P_x and P_y differ by four orders of magnitude. P_y is so small that it is negligible. In core A, the output light has only x-polarized mode. Figure 7b shows that the normalized power in core B depends on the propagation distance, and the curves follow the law of sine function. When the propagation distance is $103 \mu\text{m}$, P_x is 0.00009 and P_y is 0.99994. In core B, the output light has only y-polarized mode. By the polarization splitter, the output light is separated into x-polarized light in core A and y-polarized light in core B.

Fig. 7 Normalized output power varies with the propagation distance, **a** in core A, **b** in core B



Figures 4, 5, 6 and 7 show the simulation results when the wavelength of incident light is 1.55 μm . When the incident wavelength changes, L_x and L_y vary with the wavelength, resulting in the variations of P_x and P_y . Figure 8 shows the changes in P_x and P_y with wavelength.

The performance of the polarization splitter can be assessed by the extinction ratio (ER). The extinction ratio in core A is denoted by ER_A and the extinction ratio in core B is denoted by ER_B . Figure 9 shows ER_A and ER_B vary with wavelength. ER_A is less than -20 dB within the range of 1.458–1.635 μm . The minimum value of ER_A is -73 dB, which appears at 1.55 μm . ER_B is less than -20 dB within the range of 1.508–1.587 μm . The minimum value of ER_B appears at 1.53 μm . At the wavelength of 1.55 μm , ER_B is -45 dB.

3.3 Insertion loss

When designing an optical communication device, the insertion loss (IL) is also a parameter must be considered. IL is defined as (Khaleque and Hattori 2015)

$$IL = -10\log_{10}\left(\frac{P_{out}}{P_{in}}\right) \tag{6}$$

Fig. 8 Normalized output power varies with wavelength **a** in core A, **b** in core B

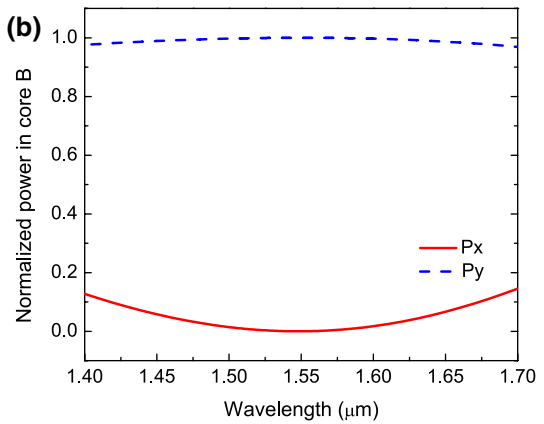
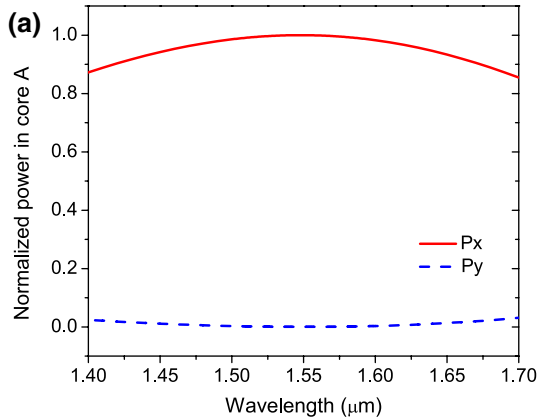


Fig. 9 Extinction ratio varies with wavelength **a** in core A, **b** in core B

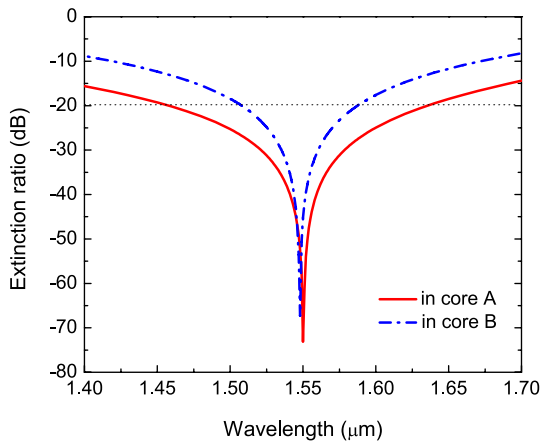
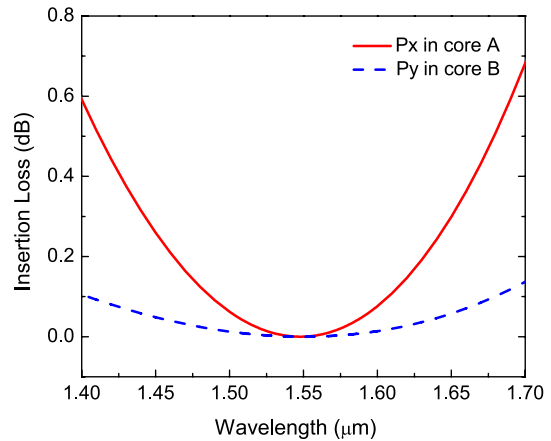


Figure 10 shows that the insertion loss of x -polarized mode in core A (denoted by IL_x) is larger than the insertion loss of y -polarized mode in core B (denoted by IL_y). In the working bandwidth (1.508–1.587 μm), the maximum value of IL_x is 0.043 dB, the maximum value of IL_y is 0.009 dB. At 1.55 μm , IL_x is 0.00013 dB, IL_y is 2×10^{-7} dB.

Fig. 10 Insertion loss varies with wavelength**Table 1** Comparison of the parameters of DC-PCF polarization splitters. (Reproduced with permission from Fan et al. 2015; Khaleque et al. 2015; Liu et al. 2017)

PCFs	Device length (μm)	ER_A (dB)	ER_B (dB)	Band width (dB)	IL_x (dB)	IL_y (dB)
Fan et al. (2015)	542	- 84	- 46	210	1.01	1.5
Khaleque et al. (2015)	117	- 100		460	0.844	1.165
Liu et al. (2017)	510	20		284	0.13408	
Younis et al. (2018)	5678	- 30		3	0.2	
Prop. PCF	103	- 73	- 45	177	0.00013	2×10^{-7}

The parameters comparing with other polarization splitters are shown in Table 1. In Refs. Fan et al. (2015), Khaleque et al. (2015), the addition of gold in PCF excites surface plasmon resonance (SPR). Adding gold to the PCF can reduce the coupling length of the two polarization modes and shorten the split distance, but at the same time it also increase the insertion loss of the polarization beam splitter. The reason is part of the light field energy transfers to the metal surface, and dissipates through the heat generation. Compared to Fan et al. (2015), Khaleque et al. (2015), not only does our splitter have a short length, but also ultra-low insertion loss. In Ref. Liu et al. (2017), Younis et al. (2018), PCFs are selectively filled by tellurite glass and NLC material. Compared to Liu et al. (2017), Younis et al. (2018), our splitter has a shorter length, better extinction ratio and smaller insertion loss.

4 Conclusions

In this paper, a novel polarization splitter based on dual-core photonic crystal fiber is investigated. By introducing a channel for energy transmission, the polarization splitter has a short length of only 103 μm. At the wavelength of 1.55 μm, the extinction ratios of core A and core B reach 73 and 45 dB, and the bandwidth with extinction ratio less than - 20 dB

are 177 and 79 nm. Moreover, the insertion loss of x-polarization mode is 0.00013 dB and the insertion loss of y-polarization mode is 2×10^{-7} dB.

Acknowledgements This work was supported by the National Natural Science Foundation of China (Grant Nos. 61475134 and 61505175) and the Science Research Projects of Hebei Province, China (Grant Nos. 17210404, Z2017056 and BJ2017108) and Science & Technology Project of Tangshan City (Grant No. 17110218a).

References

- Fan, Z., Li, S., Zhang, W., et al.: Analysis of the polarization beam splitter in two communication bands based on ultrahigh birefringence dual-core tellurite glass photonic crystal fiber. *Opt. Commun.* **333**, 26–31 (2014)
- Fan, Z., Li, S., Liu, Q., et al.: Plasmonic polarization beam splitter based on dual-core photonic crystal fiber. *Plasmonics* **10**(6), 1283–1289 (2015)
- Florous, N., Saitoh, K., Koshiba, M.: A novel approach for designing photonic crystal fiber splitters with polarization-independent propagation characteristics. *Opt. Express* **13**(19), 7365–7373 (2005)
- Geng, P., Zhang, W., Gao, S., et al.: Orthogonal single-polarization single-core photonic crystal fiber for wavelength splitting. *Photon. Technol. Lett.* **24**(15), 1304–1306 (2012)
- Jiang, H., Wang, E., Zhang, J., et al.: Polarization splitter based on dual-core photonic crystal fiber. *Opt. Express* **22**(25), 30461–30466 (2014)
- Khaleque, A., Hattori, H.: Polarizer based upon a plasmonic resonant thin layer on a squeezed photonic crystal fiber. *Appl. Opt.* **54**(9), 2543–2549 (2015)
- Khaleque, A., Mironov, E., Hattori, H.: Analysis of the properties of a dual-core plasmonic photonic crystal fiber polarization splitter. *Appl. Phys. B* **121**(4), 523–532 (2015)
- Li, P., Zhao, J.: Polarization-dependent coupling in gold-filled dual-core photonic crystal fibers. *Opt. Express* **21**(5), 5232–5238 (2013)
- Li, D., Zhou, G.: Theoretical simulation of a novel birefringent photonic crystal fiber with surface plasmon resonance around 1300 nm. *Chin. Phys. B* **25**(3), 034209 (2016)
- Liu, Q., Li, S., Fan, Z., et al.: Numerical analysis of high extinction ratio photonic crystal fiber polarization splitter based on ZnTe glass. *Opt. Fiber Technol.* **21**, 193–197 (2015)
- Liu, Q., Li, S., Gao, X., et al.: Simulation of a short and broadband polarization splitter based on photonic crystal fiber filled with tellurite glass. *Opt. Quantum Electron.* **49**(2), 1–9 (2017)
- Miliou, A., Srivastava, R., Ramaswamy, R.: A 1.3 μm directional coupler polarization splitter by ion exchange. *J. Lightwave Tech.* **11**(2), 220–225 (1993)
- Nagasaki, A., Saitoh, K., Koshiba, M.: Polarization characteristics of photonic crystal fibers selectively filled with metal wires into cladding air holes. *Opt. Express* **19**(4), 3799–3808 (2011)
- Peng, G., Tjugiarto, T., Chu, P.: Polarisation beam splitting using twin-elliptical-core optical fibres. *Electron. Lett.* **26**(10), 682–683 (1990)
- Schmidt, M., Sempere, L., Tyagi, H.: Waveguiding and plasmon resonances in two dimensional photonic lattices of gold and silver nanowires. *Phys. Rev. B* **77**(3), 033417 (2008)
- Wu, C., Wu, T., Chang, H.: A novel fabrication method for all-fiber weakly fused polarization beam splitters. *IEEE Photon. Techn. Lett.* **7**(7), 786–788 (1995)
- Wu, J., Zhou, C., Cao, H., et al.: Broadband polarizing beam splitter with metal-wire nanograting in near infrared region. *Opt. Layer Technol.* **47**, 166–170 (2013)
- Yogalakshmi, S., Selvendran, S., Sivanantha, R.: Design and analysis of a photonic crystal fiber based polarizing filter using surface plasmon resonance. *Laser Phys.* **26**(5), 056201 (2016)
- Younis, B., Heikal, A., Hameed, M., et al.: Highly wavelength-selective asymmetric dual-core liquid photonic crystal fiber polarization splitter. *JOSA B* **35**(5), 1020–1029 (2018)